

# Parameter-Efficient Deep Learning for Ultrasound-Based Human-Machine Interfaces <sup>\*</sup>

Antonios Lykourinas<sup>1</sup>, Chinmay Pendse<sup>2,3</sup>, Francky Catthoor<sup>4</sup>, Veronique Rochus<sup>3</sup>, Xavier Rottenberg<sup>3</sup>, and Athanassios Skodras<sup>1</sup>

<sup>1</sup> Dept. of ECE, University of Patras, Patras, Greece  
{alykourinas,skodras}@ac.upatras.upatras.gr

<sup>2</sup> Katholieke Universiteit (KU) Leuven, Leuven, Belgium  
<sup>3</sup> Imec, Leuven, Belgium

{Chinmay.Pendse,Veronique.Rochus,Xavier.Rottenberg}@imec.be

<sup>4</sup> Dept. of ECE, National Technological University of Athens, Athens, Greece  
catthoor@microlab.ntua.gr

**Abstract.** Ultrasound (US) has emerged as a promising modality for Human-Machine Interfaces (HMIs), with recent research efforts exploring its potential for Hand Pose Estimation (HPE). A reliable solution to this problem could introduce interfaces with simultaneous support for up to 23 degrees of freedom encompassing all hand and wrist kinematics, thereby allowing far richer and more intuitive interaction strategies. Despite these promising results, a systematic comparison of models, input modalities and training strategies is missing from the literature. Moreover, there is only one publicly available dataset, namely the Ultrasound Adaptive Prosthetic Control (Ultra-Pro) dataset, enabling reproducible benchmarking and iterative model development. In this paper, we compare the performance of six different deep learning models, selected based on diverse criteria, on this benchmark. We demonstrate that, by using a step learning rate scheduler and the envelope of the RF signals as input modality, our 4-layer deep UDACNN surpasses XceptionTime’s performance by 2.28 percentage points while featuring 87.52% fewer parameters. This result (77.72%) constitutes an absolute improvement of 0.88% from previously reported baselines. According to our findings, the appropriate combination of model, preprocessing and training algorithm is crucial for optimizing HMI performance.

**Keywords:** Ultrasound · Human-Machine Interfaces · Hand Gesture Recognition · Hand Pose Estimation

## 1 Introduction

In daily life, humans interact with machines through interfaces such as keyboards, mice, touch screens, buttons, and controllers. We refer to them collectively by using the umbrella term Human-Machine Interfaces (HMIs). Beyond

---

<sup>\*</sup> Supported by IMEC.

their role in everyday human-machine interaction, HMIs have been introduced into a wide range of domains, including rehabilitative and assistive technologies in medicine, robotic arm control and tele-operation in industry, and extended reality controllers in entertainment [4]. Nevertheless, most conventional HMIs suffer from communication bandwidth limitations, as their operation is restricted to limited Degrees-of-Freedom (DoFs). For example, a mouse cursor operates in only 2 DoFs. In contrast, our hands are capable of performing dexterous movements, spanning 23 DoFs (20 hand + 3 wrist DoFs), enabling far richer and natural interaction strategies.

Hand Pose Estimation (HPE), i.e., the continuous estimation of hand joint angles, has been approached using several sensing modalities, including optical sensors (RGB, depth, Motion Capture), Inertial Measurement Unit (IMU) sensors, and wearable gloves as a means of generating robust control signals for HMIs. However, optical-based approaches often require cumbersome multi-view camera setups for effective inference, and are sensitive to occlusion and lighting conditions, while wearable gloves can restrict natural movements [12]. In contrast, non-invasive biosignal modalities, such as surface-electromyography (sEMG) and ultrasound (US), not only overcome the aforementioned limitations but also provide the only viable means of generating control signals for amputees, who number approximately 2.3 million adults in the USA alone [11].

Within the biosignal HMI community, the Hand Gesture Recognition (HGR) problem is commonly simplified to Static Hand Pose Recognition (SHPR), as this formulation covers several practical applications. However, as evidenced by sEMG research, even SHPR remains a challenging problem that has required years of extensive iterative model development to substantially improve performance. As a reference point, the first Deep Learning (DL) baseline released with the NinaPro database in 2014 reached an accuracy of only 60.70% [1]. Recent approaches, such as TraHGR [29], have reported an accuracy of 84.13% by utilizing a 100 ms temporal window. Building on prior research, recent industry efforts have introduced large-scale datasets targeting complex tasks such as keyboard typing [16] and HPE [12], attempting to push generalization boundaries across sessions, subjects, and gestures.

In recent years, US has emerged as a promising modality for HMIs due to its ability to provide musculoskeletal structure information with sub-millimeter precision and high temporal resolution [23]. US has been extensively used to tackle the SHPR problem, reporting accuracies surpassing sEMG literature results, under similar experimental setups [8, 18, 26, 30]. Furthermore, as demonstrated in several hybrid HMI studies [17, 21], US complements the electrophysiological nature of sEMG signals, offering performance enhancements when fused. In addition, the superiority of US becomes more evident in simultaneous and proportional control (SPC) tasks where US, compared to sEMG, has been able to maintain high coefficient of determination  $R^2$  values for 3 DoFs even during their simultaneous co-activation [14]. Finally, a recent study has explored the potential of US for tackling the challenging problem of HPE [17].

Despite these promising results, the broader US-based HMI community faces challenges that limit the field’s overall progress. To begin with, most studies are conducted on private datasets, often serving as a proof-of-concept for novel US acquisition systems [6, 13, 14, 22]. In addition, the existence of only a single publicly available dataset, i.e. the Ultrasound Adaptive Prosthetic Control (Ultra-Pro) dataset, renders direct one-to-one comparison with other works infeasible due to slightly different problem formulation, experimental setups, and evaluation strategies. As a consequence, opportunities for iterative model development and benchmarking across methods are limited. Finally, an often overlooked aspect is the exploration of alternative modalities, as most studies adopt standard preprocessing procedures followed in medical US imaging, with a few notable exceptions [5, 7].

Inspired by sEMG research advancements, we aim to improve the low baselines currently reported on the Ultra-Pro dataset. This experimentation is of utmost importance before scaling to large-scale datasets targeting complex tasks (e.g. HPE, keyboard typing), where extensive exploration will become much more resource- and time-intensive. In this work, we compare six deep learning (DL) models, covering diverse architectural design choices (from attention-based to convolution-based) drawn both from state-of-the-art US-based HMI and time-series classification literature, on the Ultra-Pro dataset. Our goal is to identify optimal models in terms of performance and parameter efficiency for US-based HMIs and to assess whether the primary limiting factor of performance is input modality, model architecture, or the training algorithm. Moreover, despite its small scale, Ultra-Pro provides a challenging benchmark, since it introduces an additional DoF, i.e. wrist rotation, into the SHPR problem. This SHPR extension enables improved prosthesis functionality for transradial amputees, since the combination of the selected set of static hand poses with wrist rotation reproduces hand kinematics commonly performed in Activities of Daily Living (ADL) [28]. Our experimentation lead us to a key finding: the performance of US-based HMIs is jointly affected by multiple factors such as the choice of the input modality, network, and training algorithm. Our main contributions can be summarized as follows:

1. We conduct extensive Hyperparameter Optimization (HPO) studies on six DL models, covering both state-of-the-art US-based HMI and time-series classification literature. Additionally, we provide analysis of the studies, discuss hyperparameter importance and finally, derive optimal configurations for the task of SHPR with concurrent wrist rotation.
2. We show that for standard preprocessing, XceptionTime [10] surpasses the performance of all other models on the Ultra-Pro intra-session benchmark, reaching an accuracy of 75.44%.
3. We show that the correct combination of model architecture, input modality and training algorithm is crucial for optimizing performance. In particular, XceptionTime [10] (selected for its strong performance) and UDACNN [9] (selected for its parameter efficiency) responded differently to input modality and training algorithm modifications. By using a step learning rate scheduler

and the envelope of the RF signals as the input modality, UDACNN outperformed XceptionTime by 2.28 percentage points while featuring 87.52% fewer parameters, reaching a 77.72% recognition accuracy on the Ultra-Pro intra-session benchmark. This result constitutes an absolute improvement of 0.88% from the original Ultra-Pro baselines, obtained under a well-defined reproducible benchmark, addressing several missing implementation details from the original study.

The rest of the paper is organized as follows: Section 2 introduces the methods used in our experiments. Section 3 provides a brief description of the Ultra-Pro dataset and our experimental setup. In Section 4, we present experimental results and finally, Section 5 concludes our work.

## 2 Methods

### 2.1 Models

In this paper, we evaluate the performance of six DL models on the Ultra-Pro dataset. Model selection was based on multiple criteria. First and foremost, we included models that have been previously benchmarked on Ultra-Pro [9, 25]. Furthermore, we included models that have demonstrated strong performance in US-based SHPR, under experimental setups similar to Ultra-Pro [8, 30]. In addition, we included the XceptionTime architecture due to its exceptional performance in sEMG-based recognition [10] and biomedical time-series applications [2, 15]. Finally, we included a Vision Transformer (ViT)[3] because it represents an entirely different learning paradigm compared to the previous convolutional-based approaches.

1. A ViT variant [3] tuned for US-Based HGR. In our implementation, we use fixed 2D sinusoidal positional embeddings and average the final patch representations of the transformer encoder for classification, which is performed by a single-layer linear head.
2. The A-mode Ultrasound Network (AUSNet), proposed as part of an adaptive learning algorithm to mitigate performance downgrades caused by muscle fatigue [30].
3. The Multi-branch Squeeze-and-Excitation Network (Multi-branch SE Net) proposed in a transfer learning study [8], where A-mode US signals are processed in parallel branches and features are concatenated channel-wise after the SE mechanism is applied. A two-layer MLP network is used for the final gesture prediction.
4. The XceptionTime model, originally proposed for sEMG-based HGR [10].
5. The Single-Task Convolutional Neural Network (STCNN), introduced in the original Ultra-Pro study [25].
6. The CNN model (UDACNN) proposed in our previous inter-session recalibration work [9].

For additional details, readers could refer to the original publications.

## 2.2 Tree-Structured Parzen Estimators

In our experiments, we used Tree-structured Parzen Estimators (TPE) for HPO. In contrast to Grid and Random Search, which do not incorporate feedback during optimization, TPE exploits information from previous evaluations to guide the search towards promising regions of the search space. This property makes TPE effective in large search spaces. This behavior was also observed during our ViT experimentation, where TPE outperformed Random Search by a significant margin of 3 percentage points under an identical budget of 500 evaluations. As a result, TPE was adopted in all subsequent HPO studies using settings recommended in a prior work [19].

TPE is a Bayesian optimization algorithm designed to efficiently explore complex, potentially tree-structured search spaces, i.e. search spaces with conditional parameters, and has been shown to be effective in practical HPO tasks [20]. The algorithm consists of two main phases: a warm-up phase and the main optimization loop. In the warm-up phase, hyperparameter configurations  $\mathbf{x}$  are randomly sampled from the search space and evaluated to collect initial observations  $D = \{(\mathbf{x}_i, y_i)\}_{i=1}^{N_{init}}$ , where  $y_i$  is the objective value for a given configuration  $\mathbf{x}_i$ . In the main loop, observations are split into two groups: good configurations  $D^{(l)}$  (top-performing fraction) and bad configurations  $D^{(g)}$  (rest) and parzen estimators are used to model the distributions  $p(\mathbf{x}|D^{(l)})$  and  $p(\mathbf{x}|D^{(g)})$ . The two distributions are used to construct the *acquisition function*, defined as their ratio, from which we sample candidates that are likely to improve the objective. The best candidate is included in our observations  $D$  and this process is repeated until the pre-defined budget is exhausted.

## 2.3 Learning Rate Schedulers

In this work, we also explored the use of learning rate schedulers for improving the convergence of our training algorithms. Learning rate schedulers have become an important tool in DL, since they combine both the benefits of small and large learning rates by dynamically adjusting the learning rate throughout the training process. We restricted our experimentation to two representative schedulers: an *exponential scheduler*, which decays the learning rate by a factor  $\gamma$  every epoch, and a *step scheduler*, which reduces the learning rate by a factor  $\gamma$  every  $s$  epochs. Our scheduler choices are motivated by two reasons: *i*) they involve few hyperparameters, making them easier to debug and tune and *ii*) despite their simplicity, they have been proven very effective in various domains [10].

# 3 Experimental Setup

## 3.1 Ultra-Pro

The Ultra-Pro dataset contains US, sEMG, and IMU recordings from four transradial amputee subjects [25]. As mentioned in the Introduction, Ultra-Pro is

the only publicly available dataset and targets the task of simultaneous finger gesture recognition and wrist rotation angle estimation, which constitutes a more challenging benchmark than standard SHPR formulations. Furthermore, its public availability, which enables reproducible and systematic comparisons across methods, combined with its practical relevance for functional prosthesis applications, renders Ultra-Pro the *de facto* benchmark dataset within the US-based HMI community. The dataset includes six distinct finger gestures, namely Rest (RS), Power Grip (PG), Fine Pinch (FP), Index Point (IP), Tripod Grip (TG), and Key Grip (KG), selected based on ADL and prosthetics literature. Each subject participated in three distinct sessions. In each session, subjects executed the gestures sequentially. Gesture execution involved maintaining a static hand pose for 50 seconds while concurrently performing wrist rotations at an approximate frequency of 0.5 Hz. Ultrasound data were collected using a customized armband equipped with 8 evenly spaced transducers around the forearm operating at 5 MHz, driven by a dedicated acquisition device [24]. Data from all modalities were captured simultaneously and synchronized through specialized software. For more details, we encourage readers to refer to the original publications [24, 25].

### 3.2 Data Preprocessing and Preparation

In this paper, we adopt two preprocessing configurations in order to derive two distinct input modalities for our networks. For our primary configuration, we follow the standard procedure of Time-Gain Compensation (TGC), bandpass filtering, envelope detection and log compression (TGC and log compression parameters were taken from [27]). Additionally, only in our final experiment, we investigate an alternative modality in which we directly extract the envelope of the raw RF signals. We refer to these preprocessing configurations as A-mode US and Envelope(RF). In both cases, after discarding the first and last two samples, the pre-processed signals from all channels ( $C$ ) are vertically concatenated to form the network input of size  $C \times L$ , where  $L$  is the sequence length. Finally, for fair comparison, we followed the same train-validation-test split as in the original paper [25].

### 3.3 Training Details

The task of SHPR is formulated as a classification problem. Thus, we use cross entropy loss as our loss function. Model parameters are optimized using the Adam optimizer with default settings ( $\beta_1 = 0.9, \beta_2 = 0.999$ ). Adam was selected because *i*) it was already used in the original papers and, *ii*) it is a reliable starting point for gradient-based optimization of deep learning architectures when no optimizer is specified. Finally, we chose to use a batch size of 32 throughout our experiments to balance training time with the beneficial stochasticity of gradient updates, which often improves convergence.

## 4 Results

This section outlines the structure of our experiments and the motivation behind them. Our study was conducted in three stages:

1. HPO studies for the six DL models.
2. Intra-session model performance assessment, i.e. training and testing are carried out independently for each session, followed by identification of two candidates based on performance and parameter efficiency for further experimentation.
3. Exploration of the effect of learning rate schedulers and input modality on the selected candidates.

Except for the ViT experimentation, where we had to identify optimal hyperparameters from scratch, the motivation behind the HPO studies is two-fold: *i)* identify whether the hyperparameters reported in the original papers are optimal for the Ultra-Pro experimental setup and *ii)* infer missing hyperparameters and training details that were not specified in the original papers. The HPO studies ensured a fair comparison on the Ultra-Pro intra-session benchmark, where we identify the two promising candidates (based on performance and parameter efficiency) for further experimentation. In our final experimental section, we investigate whether performance limitations arise from the training algorithm and the input modality itself, rather than the underlying model architecture. Finally, it is important to note that each individual experiment (except HPO studies) was conducted 10 times using different random seeds.

### 4.1 HPO Results

This section presents the HPO results for all six DL models. For consistency, all HPO studies were conducted using TPE with a budget of 500 trials and 50 warm-up trials. Each experiment follows the same structure: *i)* definition of the hyperparameter search space, *ii)* analysis of promising configurations and hyperparameter importance discussion, and *iii)* selection of the final configuration based on step *ii*.

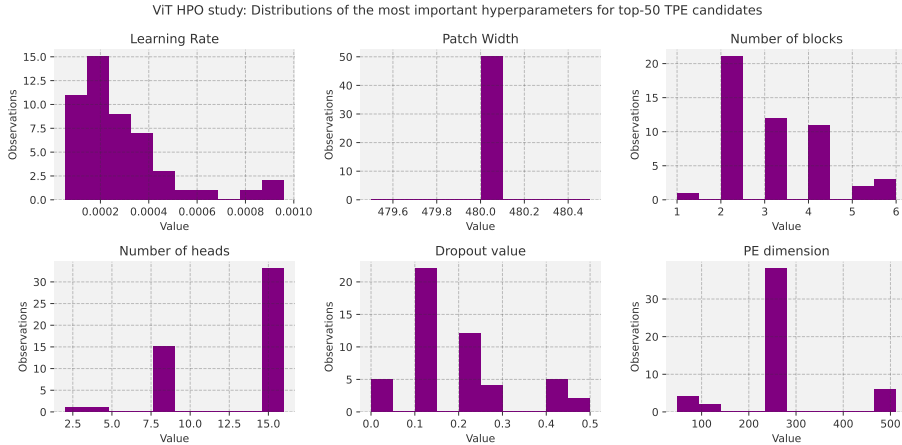
**HPO results for the ViT variants** The search space required careful design thus we restricted most hyperparameters to categorical variables, except for the learning rate and the number of epochs, for two reasons: *i)* only certain configurations can produce valid architectures (e.g. Patch Embedding (PE) dimension/image width must satisfy divisibility constraints with respect to the number of heads/patch width) and *ii)* discretizing the space reduces its effective cardinality, enabling a more efficient search. The final search space can be seen in Table 1. Note that *FFN mul* refers to the feed-forward expansion ratio, i.e., the multiplier applied to the hidden dimension of the MLP layers.

Based on our HPO analysis, we came up with the following observations:

**Table 1.** ViT: Hyperparameter Search Space for TPE HPO study

Hyperparameter	Variable Type	Range
Learning rate	float	$[1e - 5, 1e - 1]$
PE dimension	categorical	[32, 48, 64, 128, 256, 512, 1024]
Patch height	categorical	[1, 2, 4, 8]
Patch width	categorical	[4, 8, 16, 32, 64, 120, 240, 480]
Heads	categorical	[2, 4, 8, 16]
Encoder blocks	categorical	[1, 2, 3, 4, 5, 6]
FFN mul	categorical	[1, 2, 3, 4]
Epochs	Integer	[1, 200]

1. Patch width emerged as the most influential hyperparameter as TPE’s top-50 candidates were solely sampled with the largest patch width available in the search space (See Figure 1),
2. TPE also showed a clear preference towards ViTs with a relatively shallow architecture, typically between 2 and 4 encoder blocks.
3. Among the top-50 performing candidates, TPE predominantly sampled a PE dimension of 256, 16 attention heads, and a dropout rate of 0.1 (See Figure 1).
4. Over-parameterized ViT variants underperformed, indicating that increased model capacity does not necessarily improve performance. Best performing variants typically fell within a parameter range of approximately  $200k$  to  $3M$  (See Figure 2)

**Fig. 1.** ViT HPO Study: Distributions of the most important hyperparameters based on the top-50 performing candidates sampled by TPE

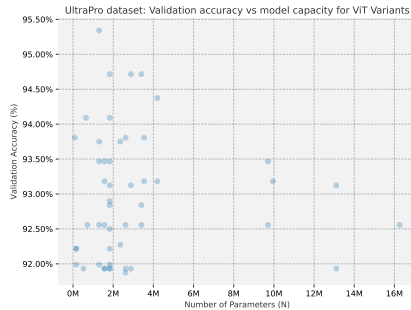


**Fig. 2.** ViT HPO Study: Scatter plot between the number of parameters and HPO objective (Validation Accuracy) for the top-50 performing candidates sampled by TPE.

The selected configuration derived from our HPO study is shown in Table 2. This model has 647,814 trainable parameters and will be referred to as USViT throughout the paper. In subsequent experiments, USViT was trained using a learning rate of 0.00048 for 57 epochs.

**Table 2.** Optimal ViT Configuration discovered through our HPO study analysis

Parameter	Patch Size	PE dimension	Heads	Encoder blocks	Dropout
Value	(2, 480)	256	16	3	0.1

**HPO results for AUSNet** The hyperparameter search focused on dropout, learning rate and number of epochs for training (See Table 3). Hyperparameters missing from the original paper [30], e.g. learning rate and number of epochs, were inferred through TPE Optimization.

**Table 3.** Search Space for the AUSNet Network

Hyperparameter	Type	Range
Learning Rate	Float	$[1e - 5, 1e - 1]$
Dropout	Categorical	$[0.0, 0.1, 0.2, 0.3, 0.3, 0.5]$
Number of Epochs	Integer	$[1, 200]$

Based on our analysis, we came up with the following observations:

1. Convergence was achieved across a wide range of learning rate values, with the best-performing candidates consistently falling within the range between 0.005 to 0.01.

2. Both dropout values of 0.2 and 0.5 supported good generalization.

The hyperparameter configuration derived from the HPO study is a learning rate of 0.0064, a dropout rate of 0.2 and 99 training epochs.

**Remaining HPO Studies Results** We briefly summarize the results from the remaining HPO studies:

- **Multi-branch SE Net:** The search focused on learning rate, dropout, number of epochs, and SE reduction ratio. Unable to discover hyperparameter configurations with satisfactory performance (best trial 86.65%). This could be attributed to the transducer operating frequency mismatch (2.25 MHz vs. 5 MHz used in all other studies), suggesting that model parameter adaptation to the new experimental setup is required.
- **XceptionTime:** The search space included solely learning rate and number of epochs. Hyperparameter configuration discovered with TPE: a learning rate of 0.0014 and 60 training epochs.

The learning rates for STCNN and UDACNN were adopted from [9]. For both models, a batch size of 32 was used. Finally, STCNN and UDACNN were trained for 30 and 60 epochs, respectively.

## 4.2 Intra-session Results

In this section, we assess the intra-session gesture recognition performance of all successfully tuned models by means of Classification Accuracy (CA) on the Ultra-Pro dataset. In contrast to the original study [25], we use our own intra-session benchmark, which is well-defined and simulates a realistic use case where the HMI needs to be operable shortly after user data have been collected [9]. Table 4 summarizes the overall results.

**Table 4.** Ultra-Pro Dataset: intra-session benchmark results. Models are presented in descending order based on their average CA.

Model	XceptionTime	USViT	UDACNN	AUSNet	STCNN
Average CA	75.44%	74.54%	74.03%	71.27%	71.26%
Trainable parameters	405,250	647,814	50,584	733,572	418,806

XceptionTime emerged as the top-performing model, achieving a accuracy of 75.44% across all subjects and sessions. Its strong performance is due to robust inter-subject generalization, particularly evident in the sessions of the third subject, which were identified as the most challenging. We attribute this ability to the use of multiple parallel depthwise convolutions in each XceptionTime module, which capture temporal patterns at multiple receptive fields without requiring pre-defining kernel sizes.

UDACNN achieves competitive performance, trailing behind XceptionTime and USViT by 1.41 and 0.51 percentage points, respectively, while using 87.52% and 92.19% fewer trainable parameters. Surprisingly, STCNN and AUSNet achieve significantly lower performance than UDACNN despite having  $14.50\times$  and  $8.28\times$  the number of its trainable parameters, respectively. This demonstrates that careful model design is more important than simply increasing capacity which can lead to overfitting.

### 4.3 Experimentation with Schedulers and Input Modality

In this section, we experiment with schedulers and input modality in an attempt to further improve the performance of XceptionTime and UDACNN models. XceptionTime was selected due to its strong and consistent inter-subject performance, whereas UDACNN was chosen for its high parameter efficiency. We first examine the impact of learning rate schedulers on the convergence behavior of both models. Additionally, we evaluate Envelope(RF) as an alternative input modality to assess whether the standard A-mode US modality constitutes a limiting factor in model performance.

**Experimentation Phase for UDACNN** By manually tuning the learning curves across different subjects and sessions of the Ultra-Pro dataset, we identified the optimal scheduler configurations. For the exponential scheduler, we used a decay factor  $\gamma = 0.9$  whereas for the step scheduler, we used a step size  $s = 10$  and a decay factor  $\gamma = 0.5$ . These scheduler configurations were adopted for both modalities. For both schedulers, an initial learning rate of 0.003 and 60 epochs were used for training.

**UDACNN Performance Comparison** We evaluate the impact of learning rate schedulers and input modality on the performance of UDACNN. Specifically, we compare training with no scheduler, an exponential scheduler, and a step scheduler, using both A-mode US and Envelope(RF) modalities. The average classification accuracies (followed the intra-session evaluation procedure) on the Ultra-Pro dataset are reported in Table 5.

**Table 5.** UDACNN: Average CA on the Ultra-Pro intra-session benchmark for different experimental configurations

	None	Exp. Scheduler	Step Scheduler
A-line Signals	74.03%	75.29%	76.51%
Envelope(RF)	75.33%	77.32%	77.72%

Based on these results, we came up with the following observations:

1. UDACNN benefits from the use of a learning rate scheduler, regardless of the input modality.

2. The Envelope(RF) modality leads to improved generalization compared to A-mode US, suggesting that additional pre-processing steps omitted in the standard configuration might be redundant or even have a negative effect on the performance of this model.
3. Combining the step scheduler with Envelope(RF) modality achieves an average recognition accuracy of 77.72%, surpassing results reported in the original work by approximately 1%, in which several implementation details are missing [25].

**UDACNN: Inter-subject compatibility of Exponential Scheduler Parameters** To assess whether the performance gains of UDACNN depend on subject-specific tuning, we evaluated the inter-subject robustness of the exponential learning rate scheduler. Session-wise hyperparameter optimization studies revealed consistent preferences for a decay factor above 0.75 across all subjects, indicating limited sensitivity to inter-subject variability. The search space also included  $\gamma = 1.0$  (i.e., no decay) to allow TPE identify whether learning rate scheduling was beneficial. The manually selected hyperparameters align well with the optimal configurations observed across sessions supporting their use as a robust, subject-agnostic choice.

**XceptionTime: Effect of Schedulers & Pre-processing** We evaluated the impact of learning rate schedulers and Envelope(RF) input modality on XceptionTime. Neither exponential nor step scheduler improved performance using A-mode US as input. Furthermore, when we used Envelope(RF), the average recognition accuracy on Ultra-Pro decreased from 75.44% to 74.77%. The degradation in performance when using the Envelope(RF) modality is potentially attributed to the loss of relative signal contrast across the dynamic range. Logarithmic compression amplifies lower-amplitude sections of the signal while compressing higher-amplitude ones. This process emphasizes subtle variations in the envelope signal that might be crucial for the XceptionTime’s convolutional filters to extract discriminative features. In contrast, Envelope(RF) preserves the full dynamic range, which makes smaller but more informative patterns less distinguishable, leading to poorer model performance. Furthermore, this observation is consistent with the original XceptionTime study [10], where the application of the  $\mu$ -law transform (another non-linear transform used for dynamic range compression) to the sEMG signals led to a substantial performance improvement, even increasing by 10% when temporal windows of 50 ms were used.

## 5 Conclusions

In this paper, we conducted a comprehensive study of six DL models, covering standard time-series classification approaches as well as models explicitly designed for US-based HGR, and assessed their performance on the publicly available Ultra-Pro dataset. We performed extensive HPO using TPE to derive

optimal configurations for each architecture and analyzed the influence of crucial hyperparameters on model performance. Furthermore, we leveraged those findings to evaluate the task-refined models in the intra-session benchmark of Ultra-Pro, where training and testing are carried out independently for each session. Finally, we selected two promising models, XceptionTime, for its strong performance and UDACNN, for its parameter efficiency and explored strategies to further improve their performance by *i*) incorporating learning rate scheduling and *ii*) examining the envelope of the RF signals as an alternative input modality. Our results indicated that when trained with vanilla Adam optimizer, XceptionTime provides the strongest baseline, achieving an overall accuracy of 75.44%, followed by USViT and UDACNN with accuracies of 74.54% and 74.03%, respectively. However, by applying a step scheduler and using the envelope RF as input we substantially improved UDACNN’s performance, raising its accuracy to 77.72%. This result constitutes an absolute improvement of 0.88% over the original Ultra-Pro baseline (for single-task models), obtained within a well-defined benchmark simulating a realistic use case. In contrast, the same modifications applied to XceptionTime degraded its performance, highlighting that training strategies and pre-processing can be critical performance factors. Overall, our findings demonstrate that UDACNN when trained using a step scheduler and Envelope(RF) as input, surpasses all evaluated DL techniques and even outperforms XceptionTime by 2.28 percentage points while featuring 87.52% fewer parameters.

## References

1. Atzori, M., Gijsberts, A., Castellini, C., Caputo, B., Hager, A.G.M., Elsig, S., Giatsidis, G., Bassetto, F., Müller, H.: Electromyography data for non-invasive naturally-controlled robotic hand prostheses. *Scientific Data* (Dec 2014)
2. Doldi, F., Plagwitz, L., Hoffmann, L.P., Rath, B., Frommeyer, G., Reinke, F., Leitz, P., Büscher, A., Güner, F., Brix, T., Wegner, F.K., Willy, K., Hanel, Y., Dittmann, S., Haverkamp, W., Schulze-Bahr, E., Varghese, J., Eckardt, L.: Detection of patients with congenital and often concealed long-qt syndrome by novel deep learning models. *Journal of Personalized Medicine* **12**(7) (2022). <https://doi.org/10.3390/jpm12071135>, <https://www.mdpi.com/2075-4426/12/7/1135>
3. Dosovitskiy, A., Beyer, L., Kolesnikov, A., Weissenborn, D., Zhai, X., Unterthiner, T., Dehghani, M., Minderer, M., Heigold, G., Gelly, S., Uszkoreit, J., Houlsby, N.: An image is worth 16x16 words: Transformers for image recognition at scale (2021), <https://arxiv.org/abs/2010.11929>
4. Esposito, D., Centracchio, J., Andreozzi, E., Gargiulo, G.D., Naik, G.R., Bifulco, P.: Biosignal-based human-machine interfaces for assistance and rehabilitation: A survey. *Sensors* **21**(20) (2021). <https://doi.org/10.3390/s21206863>, <https://www.mdpi.com/1424-8220/21/20/6863>
5. Fernandes, A.J., Ono, Y., Ukwatta, E.: Evaluation of finger flexion classification at reduced lateral spatial resolutions of ultrasound. *IEEE Access* **9**, 24105–24118 (2021). <https://doi.org/10.1109/ACCESS.2021.3056353>

6. Frey, S., Vostrikov, S., Benini, L., Cossettini, A.: WULPUS: a Wearable Ultra Low-Power Ultrasound probe for multi-day monitoring of carotid artery and muscle activity. In: 2022 IEEE International Ultrasonics Symposium (IUS). pp. 1–4 (2022). <https://doi.org/10.1109/IUS54386.2022.9958156>
7. Gao, X., Chen, X., Lin, M., Yue, W., Hu, H., Qin, S., Zhang, F., Lou, Z., Yin, L., Huang, H., Zhou, S., Bian, Y., Yang, X., Zhu, Y., Mu, J., Wang, X., Park, G., Lu, C., Wang, R., Wu, R.S., Wang, J., Li, J., Xu, S.: A wearable echomyography system based on a single transducer. *Nature Electronics* **7**(11), 1035–1046 (Nov 2024). <https://doi.org/10.1038/s41928-024-01271-4>, <https://doi.org/10.1038/s41928-024-01271-4>
8. Lian, Y., Lu, Z., Huang, X., Shangguan, Q., Yao, L., Huang, J., Liu, Z.: A transfer learning strategy for cross-subject and cross-time hand gesture recognition based on A-Mode ultrasound. *IEEE Sensors Journal* **24**(10), 17183–17192 (2024). <https://doi.org/10.1109/JSEN.2024.3382040>
9. Lykourinas, A., Rottenberg, X., Catthoor, F., Skodras, A.: Unsupervised domain adaptation for inter-session re-calibration of ultrasound-based HMIs. *Sensors* **24**(15) (2024). <https://doi.org/10.3390/s24155043>, <https://www.mdpi.com/1424-8220/24/15/5043>
10. Rahimian, E., Zabihi, S., Atashzar, S.F., Asif, A., Mohammadi, A.: Xceptiontime: A novel deep architecture based on depthwise separable convolutions for hand gesture classification. *CoRR* **abs/1911.03803** (2019), <http://arxiv.org/abs/1911.03803>
11. Rivera, J.A., Churovich, K., Anderson, A.B., Potter, B.K.: Estimating recent US limb loss prevalence and updating future projections. *Archives of Rehabilitation Research and Clinical Translation* **6**(4), 100376 (2024). <https://doi.org/https://doi.org/10.1016/j.arrct.2024.100376>, <https://www.sciencedirect.com/science/article/pii/S2590109524000892>
12. Salter, S., Warren, R., Schlager, C., Spurr, A., Han, S., Bhasin, R., Cai, Y., Walkington, P., Bolarinwa, A., Wang, R.J., et al.: emg2pose: A large and diverse benchmark for surface electromyographic hand pose estimation. *Advances in Neural Information Processing Systems* **37**, 55703–55728 (2024)
13. Sgambato, B.G., Hakami, H., Yang, X., Barsakcioglu, D.Y., Jakob, A., Fournelle, M., McGregor, A.H., Tang, M.X., Farina, D.: Towards Natural Multi-Dof Prosthetic Control with Distributed Ultrasound. In: 2024 IEEE Ultrasonics, Ferroelectrics, and Frequency Control Joint Symposium (UFFC-JS). pp. 1–6 (2024). <https://doi.org/10.1109/UFFC-JS60046.2024.10793502>
14. Sgambato, B.G., Hasbani, M.H., Barsakcioglu, D.Y., Ibáñez, J., Jakob, A., Fournelle, M., Tang, M.X., Farina, D.: High performance wearable ultrasound as a human-machine interface for wrist and hand kinematic tracking. *IEEE Transactions on Biomedical Engineering* pp. 1–10 (2023). <https://doi.org/10.1109/TBME.2023.3307952>
15. Singh, M., Prakash, P., Kaur, R., Sowers, R., Brašić, J.R., Hernandez, M.E.: A deep learning approach for automatic and objective grading of the motor impairment severity in parkinson’s disease for use in tele-assessments. *Sensors* **23**(21) (2023). <https://doi.org/10.3390/s23219004>, <https://www.mdpi.com/1424-8220/23/21/9004>
16. Sivakumar, V., Seely, J., Du, A., Bittner, S.R., Berenzweig, A., Bolarinwa, A., Gramfort, A., Mandel, M.I.: emg2qwerty: A large dataset with baselines for touch typing using surface electromyography (2025), <https://arxiv.org/abs/2410.20081>

17. Spacone, G., Frey, S., Orlandi, M., Rapa, P.M., Kartsch, V., Benatti, S., Benini, L., Cossettini, A.: Wearable and ultra-low-power fusion of EMG and A-Mode us for hand-wrist kinematic tracking (2025), <https://arxiv.org/abs/2510.02000>
18. Vostrikov, S., Anderegg, M., Benini, L., Cossettini, A.: Unsupervised Feature Extraction From Raw Data for Gesture Recognition With Wearable Ultralow-Power Ultrasound. *IEEE Transactions on Ultrasonics, Ferroelectrics, and Frequency Control* **71**(7), 831–841 (2024). <https://doi.org/10.1109/TUFFC.2024.3404997>
19. Watanabe, S.: Tree-structured parzen estimator: Understanding its algorithm components and their roles for better empirical performance. *arXiv preprint arXiv:2304.11127* (2023)
20. Watanabe, S., Awad, N., Onishi, M., Hutter, F.: Speeding up multi-objective hyperparameter optimization by task similarity-based meta-learning for the tree-structured parzen estimator (2023), <https://arxiv.org/abs/2212.06751>
21. Wei, S., Zhang, Y., Liu, H.: A multimodal multilevel converged attention network for hand gesture recognition with hybrid sEMG and A-Mode ultrasound sensing. *IEEE Transactions on Cybernetics* **53**(12), 7723–7734 (2023). <https://doi.org/10.1109/TCYB.2022.3204343>
22. Xia, W., Zhou, Y., Yang, X., He, K., Liu, H.: Toward portable hybrid surface electromyography/A-Mode ultrasound sensing for human-machine interface. *IEEE Sensors Journal* **19**(13), 5219–5228 (2019). <https://doi.org/10.1109/JSEN.2019.2903532>
23. Yang, X., Castellini, C., Farina, D., Liu, H.: Ultrasound as a neurorobotic interface: A review. *IEEE Transactions on Systems, Man, and Cybernetics: Systems* pp. 1–13 (2024). <https://doi.org/10.1109/TSMC.2024.3358960>
24. Yang, X., Chen, Z., Hettiarachchi, N., Yan, J., Liu, H.: A wearable ultrasound system for sensing muscular morphological deformations. *IEEE Transactions on Systems, Man, and Cybernetics: Systems* **51**(6), 3370–3379 (2021). <https://doi.org/10.1109/TSMC.2019.2924984>
25. Yang, X., Liu, Y., Yin, Z., Wang, P., Deng, P., Zhao, Z., Liu, H.: Simultaneous prediction of wrist and hand motions via wearable ultrasound sensing for natural control of hand prostheses. *IEEE Transactions on Neural Systems and Rehabilitation Engineering* **30**, 2517–2527 (2022). <https://doi.org/10.1109/TNSRE.2022.3197875>
26. Yang, X., Sun, X., Zhou, D., Li, Y., Liu, H.: Towards wearable A-Mode ultrasound sensing for real-time finger motion recognition. *IEEE Transactions on Neural Systems and Rehabilitation Engineering* **26**(6), 1199–1208 (2018). <https://doi.org/10.1109/TNSRE.2018.2829913>
27. Yang, X., Zhou, Y., Liu, H.: Wearable ultrasound-based decoding of simultaneous wrist/hand kinematics. *IEEE Transactions on Industrial Electronics* **68**(9), 8667–8675 (2021). <https://doi.org/10.1109/TIE.2020.3020037>
28. Yin, Z., Meng, J., Shi, S., Guo, W., Yang, X., Ding, H., Liu, H.: A wearable multisensor fusion system for neuroprosthetic hand. *IEEE Sensors Journal* **25**(8), 12547–12558 (2025). <https://doi.org/10.1109/JSEN.2025.3546214>
29. Zabihi, S., Rahimian, E., Asif, A., Mohammadi, A.: Trahgr: Transformer for hand gesture recognition via electromyography (2022), <https://arxiv.org/abs/2203.16336>
30. Zeng, J., Sheng, Y., Zhou, Z., Yang, Y., Wang, J., Xie, Q., Liu, H.: Adaptive learning against muscle fatigue for A-Mode ultrasound-based gesture recognition. *IEEE Transactions on Instrumentation and Measurement* **72**, 1–10 (2023). <https://doi.org/10.1109/TIM.2023.3301862>